Materials Science in Semiconductor Processing 103 (2019) 104610

Contents lists available at ScienceDirect

Materials Science in Semiconductor Processing

journal homepage: www.elsevier.com/locate/mssp

ZnSe and CuSe NP's by microbial green synthesis method and comparison of I-V characteristics of Au/ZnSe/p-Si/Al and Au/CuSe/p-Si/Al structures

T. Çakıcı[a,*], M. Özdal[b], Mutlu Kundakcı[c], R. Kayalı[d]

[a] Department of Electrical and Energy, Ispir Hamza Polat Vocational School of Higher Education, Ataturk University, Erzurum, Turkey
[b] Department of Biology, Atatürk University, Erzurum, Turkey
[c] Department of Physics, Atatürk University, Erzurum, Turkey
[d] Department of Energy Systems Engineering, Isparta University of Applied Sciences, Isparta, Turkey

ARTICLE INFO

Keywords:
Nanoparticles
Bacterium
CuSe
ZnSe
Thin film
Green synthesization
TEM

ABSTRACT

Bacterial synthesis of nanoparticles (NPs) is a green chemistry approach that interconnects nanotechnology and microbial biotechnology. Some types of bacteria are used for the production of these NPs. In this study, CuSe-NPs and ZnSe-NPs have been synthesized by using selected special bacterium under dark conditions and characterized by Transmission electron microscopy (TEM). The solutions of synthesized CuSe-NPs and ZnSe-NPs were distributed dropping on the glass and p-Si substrates separately and then they were dried at 65 °C. Optical properties of the ZnSe and CuSe thin films formed on glass substrates have been investigated by ultraviolet-visible spectrophotometer (UV-VIS). Structural, morphology, and chemical compositions of the fabricated ZnSe/p-Si and CuSe/p-Si structures have been determined by X-ray diffraction (XRD) and Field-emission scanning electron microscopy (FE-SEM) with energy dispersive X-ray spectroscopy (EDS) techniques, respectively. In addition, some electrical parameters of Au/ZnSe/p-Si/Al and Au/CuSe/p-Si/Al structures have been found by current-voltage (I-V) measurements at room temperature and the obtained results have been compared.

1. Introduction

Recently, nanoparticles (NPs) have a great interest due to their matchless physicochemical structures and photoluminescence, electronic, optical, and photocatalytic properties they have prominent potential applications in a wide variety fields such as nanotechnology, industry, electro-optics, optoelectronics, lasers, photovoltaic cells, light emitting diodes, and sensors [1]. Therefore, many researchers have begun to work on nanoparticles and the materials that they would use for this purpose. They studied different nanoparticles obtained from different materials and applied methods. Some of them among these researchers have studied on ZnSe and CuSe nanoparticles. These researchers have produced these nanoparticles using different systems or chemical and physical, methods. Gaoling Yang et al. have, first, developed a method to synthesize monodisperse ZnSe supraparticles via "in situ aggregation" of ZnSe nanoparticles through a simple hot-injection method and they produced ZnSe nanoparticles and made their characterizations [2]. Azam Sobhani and Masoud Salavati-Niasari have prepared via a facile hydrothermal method using chemicals and investigated their size, morphology, and chemical compositions [3]. Hsuan I. Wang et al. have produced wurtzite phase ZnSe nanoparticles from zinc blende by femtosecond pulse laser and shown that the controlling laser influence plays a vital role in the sizes of the nanoparticles [4]. In addition, there are some researchers studying the production of CuSe nanoparticles. Chong Wei Soon has produced CuSe nanoparticles in his Ph.D. study by emulsion method using many chemicals and performed their characterizations in detail [5]. Milica Petrović and et al. have CuSe thin films by the evaporation method and investigated the effect of film thickness on its optical properties [6]. As seen from these studies, the methods used for the production of the nanoparticles mentioned above are based on the chemical and physical processes. But these processes have many disadvantages such as non-ecofriendly, non-economical, non-cleanly, and toxicity and need highly advanced experimental set-ups. Therefore, researchers began to look for new methods that do not have the disadvantages mentioned above for the production of these materials and considered the biological synthesizing method as a new method that will be an eco-friendly alternative candidate instead of these methods. After this, many researchers focused on studies involving biosynthezation methods for the production of nanoparticles [7]. Some of these researchers have produced different types of nanoparticles using bacteria [8], fungi [9], enzyme [10], and plant [11].

In addition, these studies, some of the researchers have used ZnSe and CuSe nanoparticles in the heterostructures. Due to reported high

* Corresponding author.

https://doi.org/10.1016/j.mssp.2019.104610
Received 12 February 2019; Received in revised form 3 June 2019; Accepted 5 July 2019
Available online 19 July 2019
1369-8001/

efficiencies of 17.5% [12] and enabling the integration of in silicon circuits for ZnSe/p-Si heterojunction, this structure attracts special interest. On the other hand, the usage of ZnSe in this structure plays a vital role on its optical and electronic properties since the system suffers from a number of unwanted crystalline defects may be responsible for the reduction of the device lifetime [13,14].

CuSe is also important because it is used in a wide variety of devices [14–16]. The number of researchers studying the CuSe hetero-structure is very less. Venkatachalam et al. have fabricated CuSe/p-Si heterostructure applying the vacuum evaporation technique and performing its characterization they fabricated the Au/CuSe/p-Si/Al device which exhibits a strong photoresponse in the visible region [17].

Copper selenide (CuSe) is a semiconducting material, which has electrical and optical properties suitable for photovoltaic applications. It possesses the band gap of 2.15 eV, exhibiting excellent visible-light activity [18]. The other research revealed that coupling CuSe with ZnSe thin films might be a promising visible light active photocatalyst through utilizing p-n junction effect and bandgap engineering [19].

As a result, it is very difficult to fabricate directly high-quality CuSe and ZnSe nanoparticles by using the current methods mentioned above based on the homogeneous nucleation and growth mechanism. In this study, we focused on the production of ZnSe and CuSe nanoparticles via eco-friendly biosynthesizing method using a special bacterium for the first time. Also, these nanoparticles were also deposited as ZnSe and CuSe thin films on p-Si substrates and performed their characterizations. Finally, Au/ZnSe/p-Si/Al and Au/CuSe/p- Si/Al structures were fabricated and investigated their I-V characteristics.

2. Experimental procedures

2.1. Preparation of substrates

The experimental studies carried on until the fabrication of Au/ZnSe/p-Si/Al and Au/CuSe/p-Si/Al devices will be given step by step as following: Firstly, two different types of substrates (from microscope glass and p-Si glass) with sliced as 15 mm × 10 mm pieces were prepared. Two of substrates from microscope glass on which CuSe and ZnSe thin films will be formed were separated for the UV-VIS measurements and p-Si substrates on which CuSe and ZnSe thin films will be formed were separated for the other characterization measurements. Then, these substrates were cleaned separately. Firstly, p-Si substrates were cleaned as following; these substrates were decreased for 10 min, acetone, and methanol in an ultrasonic cleaner, consecutively and then etched in a sequence of H_2O:H_2O_2:HNO_3 (6:1:1) at 60 °C, 20% HF, a solution of H_2O:H_2O_2: HCl (6:1:1) at 60 °C, 20% HF. After that, the p-Si substrates were rinsed thoroughly in de-ionized water with a resistivity of 18 MΩ cm. After the surface cleaning of these substrates, the Al was thermally evaporated onto the whole backside of the p-Si substrates at a pressure of 1×10^{-5} Torr in the vacuum pump system. To obtain low resistivity back ohmic contact, the p-Si/Al structure was annealed at about 550 °C for 3 min in flowing dry nitrogen atmosphere. After completing the cleaning of p-Si substrates, we cleaned the substrates from microscope glass using piranha solution.

2.2. Production of ZnSe and CuSe nanoparticles and fabrication of Au/ZnSe/p-Si/Al and Au/ZnSe/p-Si/Al devices

In order to obtain ZnSe and CuSe nanoparticles, the selected special bacterium was used. In this case, this selected bacterium, first, was cultured in the Tryptic Soya Broth mounted on a rotating shaking system revolving with a speed 150 rpm at 30 °C for 24 h. And then this cultured bacterium was used as inoculum. This cell suspension (100 μl, OD600 1) was inoculated into two different media the Luria Bertani Broth medium (20 mL) containing 0.5 mM $CuSO_4$ + 0.5 mM Na_2SeO_3 and 0.5 mM $ZnSO_4$ + 0.5 mM Na_2SeO_3, respectively. Solutions of $CuSO_4$, Na_2SeO_3, and $ZnSO_4$ were prepared with double distilled water. All the nanoparticles biosynthesis was conducted at 30 °C for a period of 96 h on rotating shaker (150 rpm) in dark. Control experiments without Na_2SeO_3, $ZnSO_4$, and $CuSO_4$ were performed simultaneously. Then nanoparticles were obtained from the broth medium by using a procedure modified by Oremland et al. [20]. Then, cell suspensions containing NPs were sonicated in an ultrasonic bath for 10 min and centrifuged at 10,000 g for 10 min to obtain clean ZnSe and CuSe nanoparticles. After this process, cleaned ZnSe and CuSe nanoparticles were suspended in deionized water. These nanoparticles characterized by using the TEM technique.

Solutions of ZnSe and CuSe nanoparticles were dropped and distributed homogeneously on p-Si/Al and glass substrates (50cc solution) and they were dried on the hot plate at 65 °C for 60 min. Thus, ZnSe and CuSe thin films were formed on substrates. After completing these processes, it was undergoing electrode construction with gold on the upper surfaces of only p-Si substrates on which ZnSe/p-Si/Al and CuSe/p-Si/Al films were formed. This process was realized evaporating Au metal on the upper surfaces of these samples as rectifying contact with shadow mask cylindrical geometry of 1.00 mm diameter in vacuum pump ($1.5\ 10^{-5}$ Torr) fabricating Au/ZnSe/p-Si/Al and Au/ZnSe/p-Si/Al devices.

2.3. Characterization of the thin films

After completing the fabrication of the samples, we performed the characterization of the thin film samples. We determined the optical properties, crystal structures, surface morphology, and qualitative analysis of ZnSe and CuSe thin films by using UV-VIS spectrometer (PerkinElmer Lambda 2S UV-Visible spectrometer and in these measurements ZnSe and CuSe thin films formed on glass substrates were used), X-rays diffractometer (XRD Bruker D2, K_α, $\lambda = 1.54$ A, Scanning angle 70°), scanning electron (FE-SEM) (Sigma 300 Model Zeiss Gemini) and electron diffusion X-ray (EDX associated with FE-SEM), respectively. Electrical properties of the Au/ZnSe/p-Si/Al and Au/CuSe/p-Si/Al devices were investigated Keithley 2400 Picoammeter/Voltage Source Meter.

3. Results and discussion

3.1. Transmission electron microscopy (TEM) analyses of ZnSe and CuSe nanoparticles

Fig. 1 (a) and (b) show TEM images of ZnSe and CuSe nanoparticles at the race of 100 nm, respectively. In Fig. 1 (a), it can clearly see a uniform dispersion of ZnSe nanoparticles with an average particle size of about 10–25 nm. Also in Fig. 2, it can say a uniform dispersion of CuSe nanoparticles with an average particle size of about 20–45 nm. These results coincide with the literature [21,22]. The average size of CuSe nanoparticles that is provided from TEM measurements is slightly higher and more uniform than ZnSe nanoparticles. TEM investigation for the CuSe nanoparticles indicates that the nanoparticles are well separated and tend to form clusters.

3.2. Optical properties

Fig. 2 (a) and (b) show the optical absorption spectra of ZnSe and CuSe thin films measured between 300 and 1000 nm for, respectively. As seen in Fig. 2 (a) and (b), there are also two graphics seen inside two small frames taking place in these two figures. To plot these two graphics plotted $(\alpha h\upsilon)^2$ as a function of photon energy for ZnSe and CuSe thin films, we calculated the absorption coefficient, α_i, corresponding to the wavelength of the photon using the following equation:

$$\alpha = \frac{1}{d} \ln \frac{1}{T} \quad (1)$$

where d is the thickness of the sample and T is the transmission values

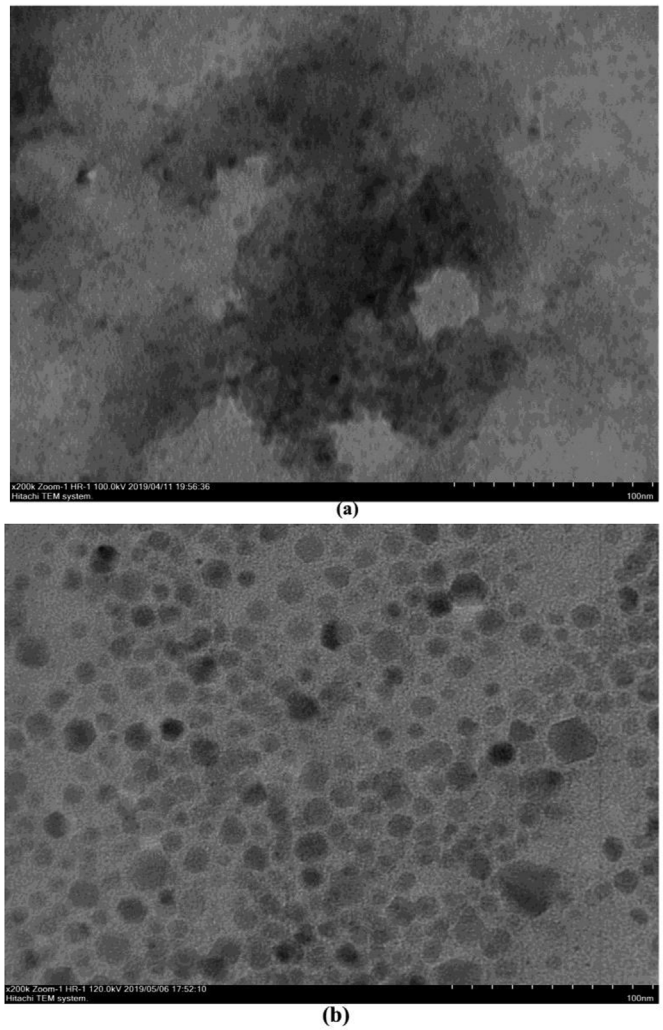

Fig. 1. TEM images of (a) ZnSe nanoparticles, (b) CuSe nanoparticles (100 nm).

obtained from absorption data corresponding to each sample. These two graphics were used to determine the optical band gap energy, Eg, values of the samples and plotted by means of the following Tauc relation [23]:

$$\alpha h\upsilon = B(h\upsilon - E_g)^n \quad (2)$$

where B, h, E_g, hυ, and n are a constant related to the effective masses of charge carriers, Planck constant, semiconductor band gap, energy of the photon, and exponent that depends on the nature of the optical transition (n = 0.5 for direct and n = 2 and for indirect transition), respectively [24]. After calculating the α as mentioned above, substituting these values and the values of the other parameters seen in Eq. (2), we plotted the graphics of $(\alpha h\upsilon)^2$ as a function of photon energy for ZnSe and CuSe thin films. To find the band gap energy, E_g, of ZnSe and CuSe thin films, we applied the extrapolation method and the intercept of the extrapolation to zero absorption with photon energy axis gave the direct band energy, Eg, values of the samples. As seen from Fig. 2 (a) and (b), the intercepts corresponding to the band gap energies of ZnSe and CuSe thin films are obtained 2.24 eV and 3.07 eV, respectively. In literature, band gap energy values of ZnSe and CuSe thin films differ from ~2.0 to 2.7 eV and ~ from 2.7 to 3.07 eV, respectively. These results are confirmed by the literature [25–30]. The band range energy values of our samples are also taking place in these regions.

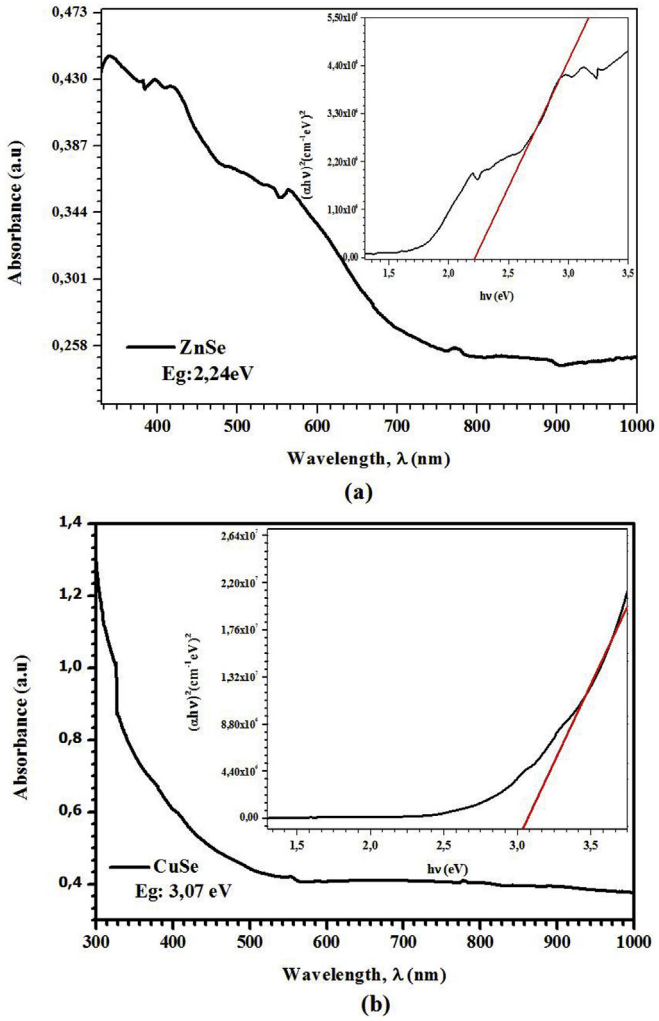

Fig. 2. Variation of optical absorbance versus the wave-length of incident photons of the as-deposited and $(\alpha h\upsilon)^2$ versus hυ plots (in small frames) corresponding to (a) ZnSe and (b) CuSe thin films.

3.3. Structural properties

Fig. 3 (a) and (b) show the XRD patterns of the ZnSe/p-Si and CuSe/p-Si structures, respectively. As seen in Fig. 3 (a), ZnSe/p-Si thin film sample having a polycrystalline structure and all orientations of the planes show that this sample has a cubic crystal structure according to the applied PDF program and JCPDS database card (PDF No:01-080-0021 and JCPDS 86–1240). On the other hand, XRD patterns of the ZnSe thin film sample depicts that the presence of two predominant planes occurs at directions (200) and (220) corresponding to the 2θ° 31 and 45.69°, respectively. As seen from Fig. 3 (b) showing the XRD patterns of CuSe/p-Si thin film sample, this sample has a polycrystalline structure as ZnSe thin film sample and all orientations of the planes show that this sample has a monoclinic hexagonal crystal structure according to the applied PDF program and JCPDS database card (PDF No:01-076-1363 and JPDS 00-049-1457). On the other hand, XRD patterns of the CuSe thin film sample reveals that the presence of two predominant planes occurs at directions (132), (102), (201), and (110) corresponding to the 2θ° 32° and 47°, respectively. Crystallite sizes of the polycrystalline corresponding to the predominant planes were evaluated by using Debye-Scherrer's formula,

$$D = 0.9\lambda/(\beta \cos\theta) \quad (3)$$

where λ is the wavelength of the X-ray (λ = 1.5405 Å) and β is the full

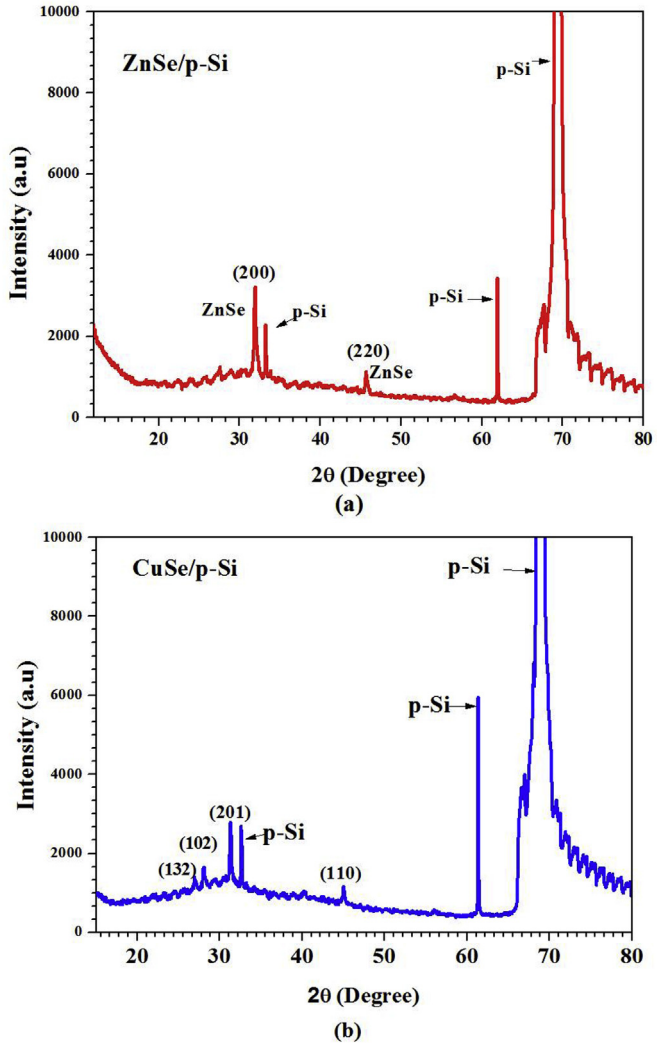

Fig. 3. XRD patterns of (a) ZnSe/p-Si and (b) CuSe/p-Si structures.

width at half maximum (FWHM) of the considered peak and θ the corresponding Bragg's angle.

The structural parameter values of the crystal sizes, D, and the distance, d, between the planes of ZnSe and CuSe thin films developed on which the p-Si substrates were formed were calculated by means of the PDF programs and the JCPDS data cards mentioned above and the obtained results were given in Tables 1 and 2. In addition, crystal sizes seen in the ZnSe thin film sample are smaller compared to the CuSe thin film sample.

The surface morphology and composition of the prepared thin film samples were studied using the images obtained from FE-SEM and EDX measurements. Fig. 4 (a) and (b) display FE-SEM images of ZnSe and CuSe thin films grown on p-Si substrates, respectively. As seen from Fig. 4 (a), FE-SEM image of ZnSe thin film sample exhibits that the surface structure of the thin film has been formed by the spherically shaped polycrystals with nanoscale, distributed rather uniformly and also the surface of the thin film is covered with these polycrystals very well.

Table 2
Crystal structural parameter values of CuSe/p-Si structure.

(hkl)	FWHM	FWHM (rad)	Intensity (a.u.)	2θ° (Observed)	d-values (nm)	Crystal size (D) nm
(130)	0.39	0.0068	248.97	27.03	3,2967	21,00
(102)	0.27	0.0047	441.38	28.09	3,1745	30,40
(201)	0.22	0.0038	1398.60	31.35	2,8514	37,51
(110)	0.27	0.0047	370.54	45.06	2,0106	31,87

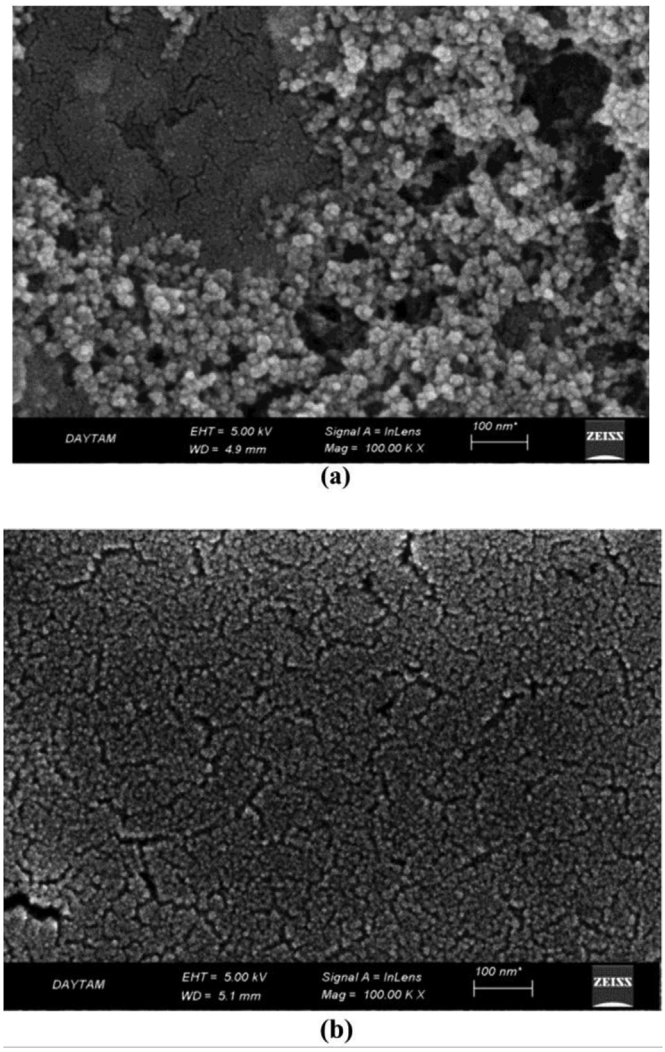

Fig. 4. FE-SEM images of (a) ZnSe/p-Si and (b) CuSe/p-Si structures with magnification scale (100 nm).

As mentioned above, the ZnSe thin film is composed of a large number of uniform spherical shaped particles and the measured average diameter of spherical particles was found varying in the range 25–50 nm. Fig. 4 (b) shows the FE-SEM image of the prepared CuSe/p-Si structure. As seen from this figure, it can be observed that the CuSe thin films are formed with the grains on which the crystallites

Table 1
Crystal structural parameter values of ZnSe/p-Si structure.

(hkl)	FWHM	FWHM (rad)	Intensity (a.u.)	2θ° (Observed)	d-values (nm)	Crystal size (D) nm
(200)	0.28	0.005	1998.99	31.96	2,7986	29,56
(220)	0.34	0.006	441.64	45.69	1,9847	25,38

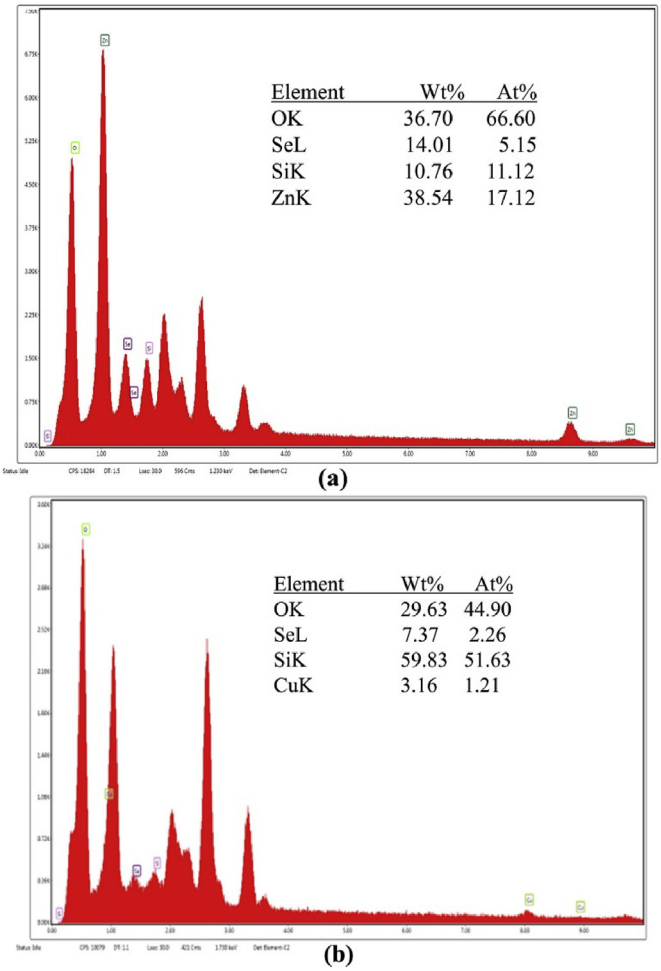

Fig. 5. EDX results of (a) ZnSe/p-Si and (b) CuSe/p-Si structures.

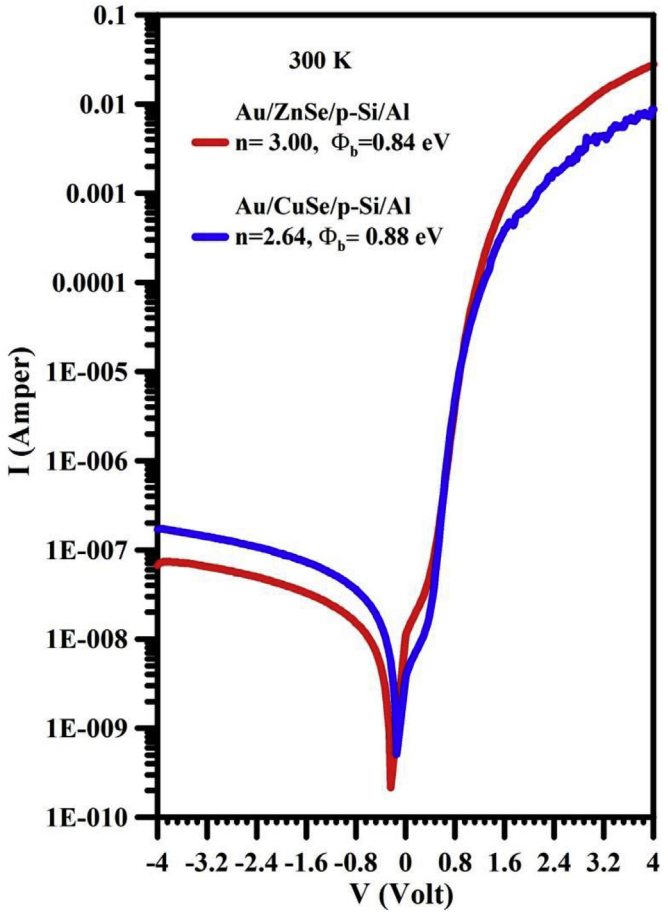

Fig. 6. I-V characteristics graphs of Au/ZnSe/p-Si/Al (red line) and Au/CuSe/p-Si/Al (blue line) devices obtained from I-V measurements carried in dark and at room temperature.

uniformly distributed and covering the substrate well. In Fig. 4 (b), it is clear that the films were composed of the single type of small densely packed nanocrystals. The grains are well defined, spherical, of almost similar size, which was uniformly distributed. The measured average diameter of spherical particles varies about 30–50 nm. These results obtained for both of ZnSe/p-Si and CuSe/p-Si structures are also confirmed by the XRD results.

The typical EDX spectra given in Fig. 5 (a) and (b) indicate the chemical composition information on ingredients in the ZnSe/p-Si and CuSe/p-Si structures, respectively. As seen in Fig. 5 (a) and (b), the elements taking place in the composition of ZnSe/p-Si and CuSe/p-Si structures and their percentages obtained from EDX measurements are given in the lists. As seen from this list, the elemental composition of the structure consists of O, Se, Zn, and Si elements in Fig. 5 (a).

These elements take place in the composition of the ZnSe/p-Si structure. As seen from this list, the elemental composition of the structure consists of O, Se, Cu, and Si elements in Fig. 5 (b).

These elements take place in the composition of the CuSe/p-Si structure. But, a small percentage of Au elements is present in the composition of these thin films. It is thought that this small amount of Au results from Au used to cover the surfaces of ZnSe/p-Si and CuSe/p-Si samples before the FE-SEM measurements.

3.4. I-V characteristics

Au/ZnSe/p-Si/Al and Au/CuSe/p-Si/Al devices whose constructions were told above were tested with I-V measurements in dark. Fig. 6 presents the I-V characteristics graph of Au/ZnSe/p-Si/Al and Au/CuSe/p-Si/Al devices obtained from experimental I-V measurements in dark and at room temperature. It was seen that these devices exhibit good rectifying properties.

In order to investigate the properties of the heterostructure devices fabricated by us, we obtained diode parameters corresponding to these devices such as ideality factor (n), barrier height (φ_b), and series resistance (R_S) calculating using by means of some theories. One of these theories is thermionic emission theory, and this theory helps to obtain ideality factor and barrier height of the diode samples from characteristics graphs of the devices obtained from I-V measurements. The current, I, included in the thermionic emission theory is given as follows:

$$I = AA^{*}T^{2}\exp\left(\frac{q\varphi_b}{nkT}\right)\left[\exp\left(\frac{qV}{nkT}\right) - 1\right] \quad (4)$$

where $I_o = AA^{*}T^{2}\exp\left(\frac{q\varphi_b}{nkT}\right)$ is the saturation current which is obtained by the intercept of the linear region at the I-V graph (Fig. 6), and also q is the charge of the electron, V is applied bias voltages, and k is Boltzmann's constant. T is the temperature at which experimental measurements were carried on, A* is the Richardson constant ($A^{*} = 32 A cm^{-2} K^{-2}$ for p-type Si) and A is an area of the diode ($=7.85 \times 10^{-3}\ cm^{2}$).

The saturation current values obtained from Fig. 6 for Au/ZnSe/p-Si/Al and Au/CuSe/p-Si/Al devices are 2.41×10^{-10} and 5.76×10^{-11} A at room temperature, respectively. On the other hand, for $V \geq 3kT/q$, the ideality factor and barrier height values of these diode samples were found from the mathematical Eqs. (5) and (6) given as follows,

$$n = \frac{q}{kT}\frac{\partial V}{\partial(\ln I)} \quad (5)$$

and

$$\varphi_b = \frac{kT}{q}\ln(AA^*T^2/I_0) \quad (6)$$

Ideality factor (n) and barrier height (φ_b) values calculated using the thermionic emission theories on characteristic I-V graphics for Au/ZnSe/p-Si/Al are 3.00 and 0.84 eV, respectively. Also, the ideality factor and barrier height values of Au/CuSe/p-Si/Al structure are found 2.64 and 0.88 eV, respectively. On the other hand, it can be said that the found higher ideality factor values in this study compared to literature results from barrier inhomogeneity and non-uniform distribution of the carriers in the interface [31].

4. Conclusion

We, first, synthesized ZnSe and CuSe nanoparticles via biosyntheses method with a special bacterium successfully and fabricated Au/ZnSe/p-Si/Al and Au/CuSe/p-Si/Al diode devices using these nanoparticles as interfacial thin films on p-Si substrates. Characterization of the ZnSe and CuSe thin films samples developed on p-Si substrates were conducted by UV-VIS, XRD, FE-SEM with EDS measurements. XRD measurements showed that ZnSe and CuSe thin films have polycrystalline structure and also have monoclinic and hexagonal crystal structures, respectively. FE-SEM images revealed that the ZnSe and CuSe thin films have nanoscale granular structure and the structures composed to expected elements checked with EDS. And also, these images showed that rather homogeneous and quality ZnSe and CuSe thin film samples were obtained successfully. On the other hand, we obtained the band gap energies of ZnSe and CuSe thin film samples as 2.24 and 3.07 eV, respectively. In addition, the fabricated Au/ZnSe/p-Si/Al and Au/CuSe/p-Si/Al diode devices by us were investigated applying I-V measurements in dark and found their ideality factors and barrier heights as 3.00 and 2.64 and 0.84 eV and 0.88 eV, respectively. And also, these I-V measurements showed that these devices have good and stable rectifying properties. As a result, we plan to apply our study for the development of the new type photodiodes and photovoltaic cells in industrial applications for the future.

References

[1] S. Hasan, A review on nanoparticles: Their synthesis and types, Res. J. Recent Sci. 1–3 (2015) 2277–2502.
[2] G. Yang, H. Zhong, R. Liu, Y. Li, B. Zou, In situ aggregation of ZnSe nanoparticles into supraparticles: Shape control and doping effects, Am. Chem. Soc. 29 (6) (2013) 1970–1976.
[3] A. Sobhani, M. Salavati-Niasari, Optimized synthesis of ZnSe nanocrystals by hydrothermal method, J. Mater. Sci. Mater. Electron. 27 (1) (2016) 293–303.
[4] H.I. Wang, W. Tsung Tang, L.W. Liao, P.S. Tseng, C.W. Luo, C.S. Yang, T. Kobayashi, Femtosecond laser-induced formation of wurtzite phase ZnSe nanoparticles in air, J. Nanomater. 2012 (2012) 278364.
[5] W.S. Chong, Synthesis and Characterization of Copper Selenide Nanoparticles via Emulsion Technique, Doctoral dissertation, UTAR), 2011.
[6] M. Petrovic, M. Gilić, J. Ćirković, M. Romčević, N. Romčević, J. Trajić, I. Yahia, Optical properties of CuSe thin films – band gap determination, Sci. of Sint. 49 (2017) 167–174.
[7] A.K. Mittal, J. Bhaumik, S. Kumar, U.C. Banerjee, Biosynthesis of silver nanoparticles: Elucidation of prospective mechanism and therapeutic potential, J. Colloid Interface Sci. 415 (2014) 39–47.
[8] P. Singh, Y.J. Kim, D. Zhang, D.C. Yang, Biological synthesis of nanoparticles from plants and microorganisms, Trends in biotech 34 (7) (2016) 588–599.
[9] M. Kitching, M. Ramani, E. Marsili, Fungal biosynthesis of gold nanoparticles: Mechanism and scale up, Microbial biotech 8 (6) (2015) 904–917.
[10] S.A. Kumar, M.K. Abyaneh, S.W. Gosavi, S.K. Kulkarni, R. Pasricha, A. Ahmad, M.I. Khan, Nitrate reductase-mediated synthesis of silver nanoparticles from AgNO3, Biotechnol. Lett. 29 (3) (2007) 439–445.
[11] J.M. Depuydt, M.A. Haase, Guha, J. Qiu, H. Cheng, B.J.Wu, G.E. Hofler, G. Meis-Haugen, M.S. Hagedorn, P.F. Baude, Room temperature II-VI lasers with 2.5 mA threshold, J. Cryst. Growth 138(1–4), 667-676.
[12] S. Guha, J.M. Depuydt, M.A. Haase, J. Qiu, H. Cheng, Degradation of II-VI based blue-green light emitters, Appl. Phys. Lett. 63 (23) (1993) 3107–3109.
[13] C. Nascu, I. Pop, V. Ionscu, E. Indra, I. Bratu, Spray pyrolysis deposition of CuS thin films, Mater. Lett. 32 (2–3) (1997) 73–77.
[14] M.A. Korzhuev, Dufour effect in superionic copper selenide, Phys. Solid State 40 (2) (1998) 217–219.
[15] V.M. Bhuse, P.P. Hankare, K.M. Garadkar, A.S. Khomane, A simple, convenient, low-temperature route to grow polycrystalline copper selenide thin films, Mater. Chem. Phys. 80 (1) (2003) 82–88.
[16] P.P. Hankare, A.S. Khomane, P.A. Chate, K.C. Rathod, K.M. Garadkar, Preparation of copper selenide thin films by a simple chemical route at low temperature and their characterization, J. Alloy. Comp. 469 (1–2) (2009) 478–482.
[17] S. Venkatachalam, S. Agilan, D. Mangalaraj, S.K. Narayandass, Short communication Optoelectronic properties of ZnSe thin films, Mater. Sci. Semicond. Process. 10 (2007) 128–132.
[18] P. Kumar, K. Singh, O.N. Srivastava, Template-free-solvothermal synthesized copper selenide (CuSe, Cu2 − xSe, β-Cu2Se and Cu2Se) hexagonal nanoplates from different precursors at low temperature, J. Cryst. Growth 312 (19) (2010) 2804–2813.
[19] W. Shi, J. Shi, S. Yu, P. Liu, Ion-exchange synthesis and enhanced visible-light photocatalytic activities of CuSe-ZnSe flower-like nanocomposites, Appl. Catal. B Environ. 138–139 (2013) 184–190.
[20] R.S. Oremland, M.J. Herbel, J. Switzer-Blum, S. Langley, T.J. Beveridge, P.M. Ajayan, T. Sutto, A.V. Ellis, S. Curran, Structural and spectral features of selenium nanospheres produced by Se-respiring bacteria, Appl. Environ. Microbiol. 70 (1) (2004) 52–60.
[21] A. Benchaabane, Z. Ben Hamed, F. Kouki, M.A. Sanhoury, K. Zellama, A. Zeinert, H. Bouchriha, Performances of effective medium model in interpreting optical properties of polyvinylcarbazole: ZnSe nanocomposites, J. Appl. Phys. 115 (2014) 134313.
[22] M.A. Malik, P. O'Brien, N. Revaprasadu, A novel route for the preparation of CuSe and $CuInSe_2$ nanoparticles, Adv. Mater. 11 (17) (1999) 1441–1444.
[23] J. Tauc, Optical Properties of Solids, North-Holland, Amsterdam, 1970.
[24] T. Çakıcı, M. Sağlam, B. Güzeldir, The comparison of electrical characteristics of Au/n-InP/In and Au/In2S3/n-InP/In junctions at room temperature, Mater. Sci. Eng. B 193 (2015) 61–69.
[25] O. Arellano-Tánori, M.C. Acosta-Enríquez, R. Ochoa-Landín, R. Iñiguez-Palomares, T. Mendívil-Reynoso, M. Flores-Acosta, S.J. Castillo, Copper-selenıde and copper-tellurıde composıtes powders sıntetızed by ıonıc exchange, Chalcogenide Lett. 11 (1) (2014) 13–19.
[26] M. Imran, Abida Saleema, Nawazish A. Khana, A.A. Khurram, N. Mehmood, Amorphous to crystalline phase transformation and band gap refinement in ZnSe thin films, Thin Solid Films 648 (2018) 31–38.
[27] G. Statkut, I. Mikulskas, A. Jagminas, R. Tomas, I. Unas, Photo-induced transmittance in copper–selenide nanowires, Opt. Mater. 30 (5) (2008) 743–745.
[28] Z. Yazar Aydın, S. Abacı, Synthesis and characterization of Cu3Se2 nanofilms by an underpotential deposition based electrochemical codeposition technique, Solid State Sci. 74 (2017) 74–87.
[29] G. Bakiyaraj, R. Dhanasekaran, Synthesis and characterization of flower-like ZnSe nanostructured thin films by chemical bath deposition (CBD) method, Appl. Nanosci. 3 (2) (2013) 125–131.
[30] B. Pejova, I. Grozdanov, Chemical deposition and characterization of Cu3Se2 and CuSe thin films, J. Solid State Chem. 158 (1) (2001) 49–54.
[31] T. Çakıcı, B. Güzeldir, M. Sağlam, Temperature-dependent of electrical characteristics of Au/n-GaAs/In Schottky diode with In2S3 interfacial layer obtained by using chemical spray pyrolysis method, J. Alloy. Comp. 646 (2015) 954–965.